PHYSICAL REVIEW D **82,** 115021 (2010)

Observing Higgs dark matter at the CERN LHC

Alexandre Alves[1]

Instituto de Física Teórica, Universidade Estadual Paulista, São Paulo, 01140-070, Brazil

(Received 13 September 2010; published 22 December 2010)

Triggering the electroweak symmetry breaking may not be the only key role played by the Higgs boson in particle physics. In a recently proposed warped five-dimensional $SO(5) \otimes U(1)$ gauge-Higgs unification model, the Higgs boson can also constitute the dark matter that permeates the universe. The stability of the Higgs boson in this model is guaranteed in all orders of perturbation theory by the conservation of an *H-parity* quantum number that forbids triple couplings to all standard model (SM) particles. Such a unique feature of the model shows up as a delay in the restoration of the tree-level unitarity, which in turn enhances the production cross section as compared to the standard model analogue. Recent astrophysical data constrain the mass of such a Higgs dark matter particle to a narrow window of 70–90 GeV range. We show that the Large Hadron Collider can observe these Higgs bosons in the weak boson fusion channel with about 260 fb^{-1} of integrated luminosity in that mass range.

DOI: 10.1103/PhysRevD.82.115021 PACS numbers: 12.10.Dm, 12.60.Cn, 95.35.+d

I. INTRODUCTION

The mechanism responsible for the breaking of the electroweak symmetry and the necessity of existence of cold dark matter (CDM) relics in the universe have motivated a large theoretical effort towards a beyond standard model (SM) physics in the last decades.

The electroweak symmetry breaking (EWSB) [1,2] is achieved in the SM and in many of its extensions, introducing scalars whose couplings to fermions and gauge bosons generate their masses. Within SM there remains a scalar particle in the spectrum: the Higgs boson. One of the major goals of the LHC is the detection and the study of the properties of the Higgs boson, which, in this respect, constitutes a window for the whole EWSB mechanism and hopefully for the high energy structure of the new physics. On the other hand, the indirect detection of the dark matter particle at colliders (whose existence has been established by the Wilkinson Microwave Anisotropy Probe (WMAP) experiment [3]) is important to establish the nature of dark matter and, again, constitute a mean to decide between new physics models.

In a recent work [4], an interesting connection between these two phenomena was proposed: the Higgs boson could also be the dark matter relic with a mass of $\sim$70 GeV in order to satisfy the constraints from WMAP [3]. In fact, the actual mass of such a particle may lie in a narrow 70–90 GeV range as shown in Ref. [5]. This connection has a deep impact in the Higgs boson phenomenology at colliders because the Higgs boson becomes absolutely stable in the warped five dimensional $SO(5) \otimes U(1)$ gauge-Higgs model proposed in Ref. [4]. As a consequence of the conservation of a new quantum number which forbids all triple couplings to SM particles (only the quartic couplings to weak bosons and fermions remain) the Higgs boson acquires a property shared by *R-parity* conserving particles of the minimal supersymmetric standard model (MSSM) [6] and *KK-parity* conserving particles from universal extra dimensions (UED) [7] scenarios for example—they are produced at colliders exclusively in pairs.

In Ref. [8], the double Higgsstrahlung channel $pp \to (W, Z)HH$ was considered at the LHC as a possible detection channel, but the backgrounds were found to be 3 orders of magnitude larger than the signal, which would demand an extremely large amount of data for detection. Associated production of Higgs and top or bottom quark is possible though $f\bar{f}HH$ is a dimension-five operator suppressed by a factor m_f/v^2, where $v = 246$ GeV is the Higgs *vacuum expectation value*. Top quark and weak boson pair production can receive contributions from quartic Higgs boson couplings but at one-loop level. Moreover, these kinds of processes must be initiated by bottom partons once the Higgs couples to mass.

In Ref. [9], the potential of the LHC to discover Higgs bosons decaying into invisible particles like gravitons, gravitinos, or neutralinos is demonstrated in the weak boson fusion (WBF) channel $pp \to jjH \to jj\not{E}_T$. In this case, the far forward tagging jets work as an experimental trigger at the same time they endow the signal events singular features that make the separation from background events possible. The discovery potential of the LHC in the WBF channel has been established for a number of SM Higgs boson decaying channels [10], Higgs bosons of the MSSM [11], and in other models [12].

Being electrically neutral, weakly interacting, and absolutely stable the detectors would miss all Higgs signals—only indirect detection would be possible via large missing momentum topologies, a typical dark matter signal at colliders. Such signals need additional charged leptons or jets, which can serve as an experimental trigger just like the invisibly decaying Higgs case of Ref. [9]. We thus propose the weak boson fusion

*aalves@fma.if.usp.br

 © 2010 The American Physical Society

$$pp \to jjHH \to jjE_T \tag{1}$$

as a potential searching channel at the LHC. The two far forward tagging jets working as the required trigger plus the large amount of missing momentum associated to the stable Higgses constitute our signal. The lack of triple couplings to SM gauge bosons delay the restoration of unitarity, which effectively occurs only when the heavy $\mathcal{O}(1)$ TeV KK gauge bosons associated to the larger gauge group $SO(5) \otimes U(1)$ start to propagate [13] resulting in an enhanced cross section compared to the SM case as we will discuss in Sec. IV.

In summary, in this work we investigate the Higgs pair production of a gauge-Higgs unification model with a high KK mass scale as proposed in Ref. [4] in the weak boson fusion channel at the 14 TeV LHC in the 70–90 GeV mass range consistent with the PAMELA, HESS, and Fermi/LAT astrophysical data as shown in Ref. [5]. Moreover, contrary to the SM case [2,13], cancellations among triple and quartic Higgs contributions do not take place until the heavy KK states start to propagate, which results in an enhanced production cross section as we discuss in Sec. II. As in the case of the single Higgs production [9], the two far forward tagging jets serve as triggers and as an efficient tool to reduce the SM backgrounds. We show that with sufficient integrated luminosity the Higgs dark matter particle of this model can be observed at the CERN LHC.

II. THE EFFECTIVE LAGRANGIAN OF THE $SO(5) \otimes U(1)$ GAUGE-HIGGS UNIFICATION MODEL

The model we are considering is a gauge theory based on the group $SO(5) \otimes U(1)$ with an warped extra-dimension [4]. The four-dimensional Higgs boson is identified with a part of the extra-dimensional component of the gauge bosons. As a consequence the Higgs couplings to all particles are fixed by the gauge principle. If the extra-dimension space is non-simply-connected the four-dimensional neutral Higgs boson will correspond to quantum fluctuations of an Aharonov-Bohm phase θ_H, which is a physical degree of freedom originated from vanishing field strengths $F_{\mathrm{MN}} = 0$.

Quantum corrections generate an effective Higgs potential $V_{\mathrm{eff}}(\theta_H)$ which depends on the Aharonov-Bohm phase θ_H along the fifth dimension. It has been shown that the effective potential has a global minimum at $\theta_H = \pm\pi/2$ [4]. Small fluctuations around the minimum $\theta_H = \pi/2 + H(x)/v$ introduce the Higgs field H responsible for the electroweak symmetry breaking.

Mirror reflection symmetry in the fifth dimension and the invariance under transformations of the larger group implies that the effective Higgs potential must be invariant under $H \to -H$. The Higgs field is odd under the H-parity transformations while all other SM particles remain even.

For our studies the relevant effective four-dimensional interaction Lagrangian of the $SO(5) \otimes U(1)$ gauge theory in the five-dimensional warped spacetime incorporating all those symmetries is given by

$$\begin{aligned}\mathcal{L}_{\mathrm{eff}} = {} & \frac{g^2 v}{2}\cos(\theta_H) W_\mu W^\mu H + \frac{g^2 v}{8c_W^2}\cos(\theta_H) Z_\mu Z^\mu H \\ & + \frac{g^2}{4}\cos(2\theta_H) W_\mu W^\mu HH \\ & + \frac{g^2}{8c_W^2}\cos(2\theta_H) Z_\mu Z^\mu HH \\ & + \sum_f \frac{m_f}{2v^2}\cos(2\theta_H)\bar{\psi}_f \psi_f HH. \end{aligned} \tag{2}$$

As a consequence of the conservation of the H parity all triple vertices involving Higgs interactions vanish at $\theta_H = \pi/2$. Only quartic interactions with SM strength survive and the Higgs boson becomes absolutely stable.

Note that the vanishing of ZZH coupling evades the LEP bound on the Higgs mass. As a matter of fact, all possible collider constraints on the Higgs mass are evaded. Nonetheless, mass bounds from WMAP, PAMELA, HESS, and Fermi/LAT allow a narrow 70–90 GeV [5] window for collider searches.

III. SEARCH STRATEGY AT THE CERN LHC AND CALCULATIONAL TOOLS

The two far forward hard jets plus missing energy topology have already been studied in the literature at the leading order for a single invisibly decaying Higgs boson production in weak boson fusion [9]. The backgrounds are exactly the same and the whole analysis can be done along the same lines. For this reason, we use the results and discussions for the backgrounds analysis from that work and simulate only the signal events for $pp \to jjHH \to jjE_T$.

The backgrounds consist of process leading to two jets and missing transverse momentum: (1) QCD and WBF $Zjj \to jj\nu\bar{\nu}$, (2) QCD and WBF $Wjj \to jj\ell\nu$, where the charged lepton is not identified, (3) QCD multijet production with large missing momentum generated by energy mismeasurements or high transverse momentum particles escaping detection through the beam-hole.

Our signal was simulated at parton level with full leading order tree-level matrix elements and full Cabibbo-Kobayashi-Maskawa matrix using the Calchep package [14] including electroweak and QCD contributions. The electroweak contributions consist of genuine WBF diagrams and double Higgsstrahlung diagrams with a Z or W boson decaying into jets as can be seen at Fig. 1. The QCD contributions are initiated by gluons, light or bottom partons, and the Higgses are radiated off the final state bottom quarks. The background events were simulated at parton level with full tree-level matrix elements using the

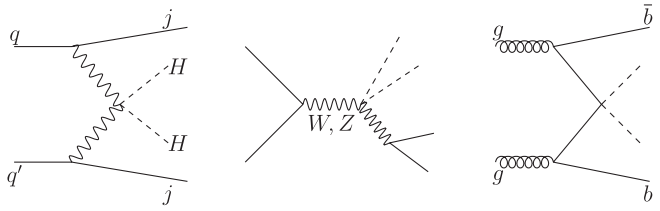

FIG. 1. Feynman diagrams contributing to the $pp \to jjHH$ process. From left to right, we show the WBF, double Higgsstrahlung, and the gluon fusion QCD contribution, respectively. There are additional QCD diagrams not shown in the figure initiated by $q\bar{q}$, $gb(\bar{b})$, and $b\bar{b}$.

MADEVENT package [15] (see Ref. [9]). Next-to-leading-order QCD corrections to the Higgs pair production in WBF process were calculated at [16], and a very modest K factor around 1 was found.

We do not take into account the contributions from the heavier KK modes of gauge bosons since we expect they will unitarize the scattering amplitudes only at some higher scale as discussed in Sec. IV. Instead, we used the unitarization prescription suggested at Ref. [17] in order to mimic the effect of the heavy KK gauge bosons at the $\mathcal{O}(1)$ TeV scale relevant for the LHC phenomenology. Yet, the WBF cross section for the model under consideration is expected to be larger than the SM analogue.

In order to be consistent with the simulations performed in Ref. [9], we employed CTEQ4L parton distribution functions [18] at the factorization scale $\mu_F = \min(p_T)$ of the defined jets. The electroweak parameters $\sin^2\theta_W = 0.23124$, $\alpha_{\rm em} = 1/128.93$, $m_Z = 91.189$ GeV, and $m_W = 79.95$ GeV were taken from Ref. [9] as well. We simulate experimental resolutions by smearing the energies (but not directions) of the defined jets with a Gaussian error given by $\Delta E/E = 0.5/\sqrt{E} \oplus 0.02$ (E in GeV).

We checked that all kinematic distributions used to impose cuts on the final states jets and missing momentum in our case are very similar to those of $pp \to jjH$ of Ref. [9]. Therefore, we can assume the same strategy to suppress the backgrounds and impose the same cuts

$$\begin{aligned} p_{T_j} &> 40 \text{ GeV} & |\eta_j| &< 5.0 \\ |\eta_{j_1} - \eta_{j_2}| &> 4.4 & \eta_{j_1} \cdot \eta_{j_2} &< 0 \\ \not{p}_T &> 100 \text{ GeV} & m_{jj} &> 1200 \text{ GeV} \end{aligned} \quad (3)$$

The cuts on the transverse momentum and rapidity of the defined jets are the standard WBF selection cuts, while the missing momentum cut explores the features of our signal with two final state dark matter particles. A very large cut on the invariant mass of the two tagging jets m_{jj} helps to reduce the backgrounds further.

The jets from the double Higgsstrahlung contributions (see Fig. 1) are on the W or Z mass shell being eliminated after the jets invariant mass cut is applied, remaining only the genuine WBF contributions. The QCD contributions $gg(q\bar{q}) \to b\bar{b}HH$, $b\bar{b} \to ggHH$, $gb(\bar{b}) \to gb(\bar{b})HH$ involve double Higgs radiation from the bottom quark lines, which are suppressed by $m_b/2v^2$ [see Eq. (2)]. Moreover, the jets from this class of contributions are typically central and softer than the jets from WBF contributions being negligible after imposing the cuts. The large SM QCD backgrounds are strongly reduced after the missing momentum cut is applied. A survival probability associated to a central soft jet activity veto of 0.28 for QCD processes, as estimated in [19] and used in Ref. [9], is crucial to reduce these backgrounds and enhance the signal to background ratio. Yet, they are ineffective against the SM WBF processes whose survival probability is high: 0.82.

For this reason the dominant background contribution after the cuts (3) is the standard model WBF contribution [9]. To suppress this background, the following cut on the azimuthal angle between the tagging jets, ϕ_{jj}, was proposed in Ref. [9]

$$\phi_{jj} < 1\,. \quad (4)$$

It explores the nature of the particle being produced between the tagging jets: a scalar (Higgs) for the signal and a vector (W, Z boson) for the background. The spin of this particle determines the angular distributions of the tagging jets and eventually of the products of their decays.

Next we discuss the tree-level unitarity violation in the $WW \to HH$ scattering and unitarization prescription used to compute a reliable cross section for the $pp \to jjHH$ process.

IV. TREE-LEVEL UNITARITY VIOLATION IN $WW \to HH$ SCATTERING

The lack of the triple couplings $(W, Z)HH$ and HHH causes the violation of tree-level unitarity of the $WW \to WW$ scattering at $\mathcal{O}(1)$ TeV [13]. The scattering amplitudes take the largest values precisely at $\theta_H = \pi/2$ in warped spacetimes in these classes of models as shown in Ref. [13]. The $\mathcal{O}(E^2)$ terms which cause the unitarity violation are cancelled as soon as the heavier KK modes of gauge bosons start to propagate, leading to a constant behavior of the amplitudes as a function of the energy E at a scale around $\mathcal{O}(10)$ TeV [13] if the KK mass scale is $m_{\rm KK} \gtrsim 1$ TeV. That is the reason why we expect the double Higgs dark matter production has a much larger cross section in the weak boson fusion channel as compared to the SM case at $\mathcal{O}(1)$ TeV scale. The WBF process is intimately related to the EWSB, and the violation or the delay in the restoration of tree-level unitary of the $WW \to WW$ scattering is a sign that new physics must come into play [20].

In the case of $W_L W_L \to HH$ scattering the S-wave amplitude gives the dominant contribution for the energies of interest

$$a_0 = \frac{1}{64\pi}\int_{-1}^{1} -i\mathcal{M}(W_L W_L \to HH) d\cos\theta = \frac{\alpha_{\rm em}}{32\sin^2\theta_W m_W^2}(M_{HH} - 2m_W^2), \quad (5)$$

where θ is the polar angle of the scattered Higgs boson in the lab frame, and $M_{HH} = (p_H + p_H)^2 = (p_{W^+} + p_{W^-})^2$ is the HH center-of-mass energy square. Unitarity of the scattering amplitude requires that $|\mathrm{Re}a_0| \leq 1/2$, which in turn implies

$$M_{HH} < 22 m_W \approx 1.8 \text{ TeV} \quad (6)$$

in agreement with the scale at which $W_L W_L \to W_L W_L$ unitarity is violated, as shown in [13].

The growth in the scattering cross section as a function of M_{HH} for $W_L W_L \to HH$ can be seen from the solid line of Fig. 2. As soon as the KK modes of the heavy gauge bosons start to propagate, the cross section should cease to increase, becoming flat at very high energies. The dashed line shows the regularized cross section as a function of M_{HH} using the elastic scattering prescription proposed in Ref. [17] replacing a_0 by $a_0/(1 - ia_0)$ in the calculation of the amplitude in order to mimic the regularizing effect of the KK states.

However if the KK mass scale is expected to be of order 1 TeV or higher, the impact on the $W_L W_L \to HH$ should be small once the phase space to produce heavy on shell KK states is restricted. To confirm that expectation, we show at the Fig. 3 the invariant mass distribution for the Higgs pair in the $pp \to jjHH$ process. We see that $d\sigma/dM_{HH}$ peaks around 300 GeV only being very small at $2m_{\rm KK} \sim$ 1.8 TeV. In fact only 5% of all events present a Higgs pair invariant mass above the unitarity threshold of 1.8 TeV. Yet, their contribution to the scattering amplitude might be important near the violation threshold energy. The dashed histogram at Fig. 3 represents the unitarized

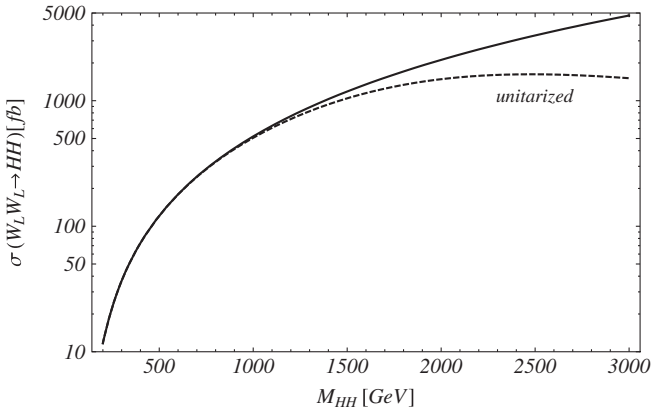

FIG. 2. The $W_L W_L \to HH$ cross section as function of the Higgs pair invariant mass. The solid line shows the nonunitarized cross section and the dashed line the cross section unitarized according to the elastic scattering prescription discussed in the text.

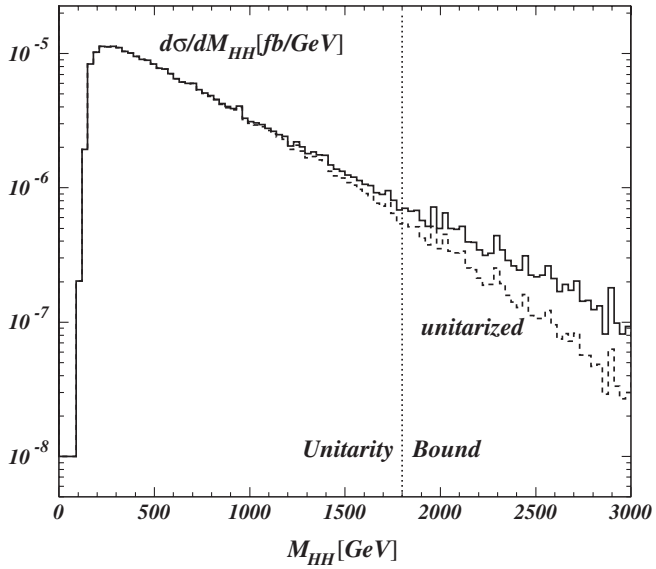

FIG. 3. The Higgs pair invariant mass distribution for the process $pp \to jjHH$. The solid histogram represents the nonunitarized distribution and the dashed histogram the unitarized one. Only 5% of all events lies above the unitarity violation threshold scale of 1.8 TeV.

distribution confirming our expectation of the small impact of the heavy KK states at the energy scale relevant for our studies. After unitarization, the total cross section decreases by a modest factor of 0.965, which was taken into account in the subsequent analysis.

V. RESULTS AND DISCUSSIONS

The signal total cross section without cuts is 29.05(27.3) fb for a 70(90) GeV Higgs boson at the 14 TeV LHC, while the total background cross section amounts to 2.79 pb. As we anticipated in Sec. II, the $pp \to jjHH$ rate in this gauge-Higgs unification model is about 5 times larger than its SM analog, whose WBF production cross section for a 70 GeV Higgs mass is 6.3 fb. The same set of parameters, factorization scale, and parton distribution functions for the Higgs dark matter case were used in this computation.

After applying all the basic cuts (3) and the ϕ_{jj} cut, and assuming the same survival probability for a central soft jet veto of $P_{\rm surv} = 0.87$ for our signal as in Ref. [9], we found 4.05(4.03) fb for the signal against 167 fb for the total background for a 70(90) GeV Higgs boson mass. Based on these rates a 5σ significance observation is possible with 255(257 fb^{-1}) of integrated luminosity for a 70(90) GeV Higgs dark matter particle. The Table I summarizes our results.

We show in Fig. 4 the normalized distributions for the ϕ_{jj} variable for our double Higgs signal, the single invisibly decaying Higgs, and the total background after applying the cuts from Eq. (3). The effect of the spin nature of

TABLE I. Signal and background cross sections after basic cuts (3), and basic cuts plus the ϕ_{jj} cut of Eq. (4). The survival probability after a soft central jet veto is incorporated already as discussed in Sec. III. We show the results for a 70 and a 90 GeV Higgs boson. The last column displays the required integrated luminosity for a 5σ significance observation.

σ(fb)	signal: $m_H = 70(90)$ GeV	Total background	$\mathcal{L}$ (fb^{-1})
basic cuts (bc)	9.7(9.3)	918	246(267)
$bc + \phi_{jj} < 1$	4.05(4.03)	167	255(257)

the particles being produced is evident from this plot and motivates the cut (4) devised to suppress the SM weak boson fusion background.

The impact of the ϕ_{jj} cut (4) on the double Higgs production is fairly the same as the single Higgs process representing a dilution factor of 0.37 in our case and 0.40 in the single Higgs case. The backgrounds on their turn are suppressed by a factor of 0.18, which motivates the cut in the single Higgs case after all. The impact of this cut on the required luminosity is mild, though changing the required integrated luminosity for a 5σ observation from 246(267 fb^{-1}) to 255(257 fb^{-1}) to a 70(90) GeV Higgs.

As suggested in Ref. [9], an analysis based on the shape of the ϕ_{jj} distribution could be a good idea to separate signal from backgrounds, but the reduced signal cross section after cuts in our case is a challenge for that purpose. It indicates that there is still some room for an optimum choice of cuts, for example, tightening the missing p_T or

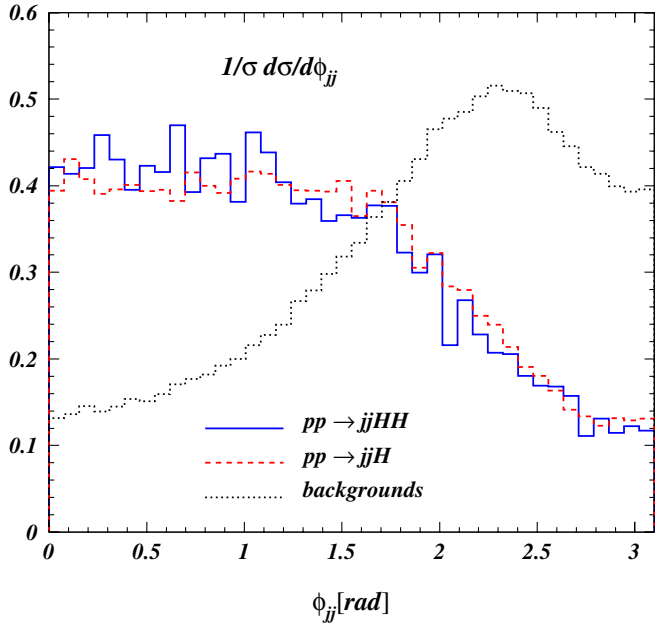

FIG. 4 (color online). The normalized distributions of the azimuthal angle separation between the tagging jets for the double Higgs ($pp \to jjHH$), single Higgs ($pp \to jjH$), and total background after applying the cuts (3).

the jets invariant mass cut. On the other hand, a complete simulation taking into account hadronization, pile-up effects, and more realistic detector efficiencies is necessary in order to evaluate the LHC potential more precisely.

An interesting question arisen looking at the ϕ_{jj} distribution of Fig. 4 is how to discriminate between a Higgs dark matter of the classes of models under consideration and a single Higgs decaying to an invisible final state with a large branching ratio as considered in Ref. [9]. It is evident it cannot be done based on the kinematic distributions of the jets. Observing signals associated to a single invisible Higgs boson production in other channels would be important for that task once we do not expect seeing signals for the classes of models we consider here based on our results and on the results from Ref. [8] as well.

Another possibility is to probe the high energy growth of the longitudinal vector boson scattering using dedicated techniques for hadron colliders as those proposed in Refs. [20,21], for example. A future linear collider could do that job easily in the WBF channel once the energy of the incoming leptons can be tuned.

It is worth mentioning that dark matter production in weak boson fusion is not likely to occur at hadron colliders in the framework of models presenting CDM candidates like the MSSM or UED, for example. In the MSSM case, it has been shown [22] that destructive interference between WBF-type diagrams and bremsstrahlung diagrams contributing to the lightest neutralino production decreases the rates to an attobarn level for $pp \to jj\tilde{\chi}^0\tilde{\chi}^0$ at the LHC. On the other hand, in the UED models, the lightest KK particle is an almost pure $U(1_Y)$ gauge boson, which strongly suppresses the couplings to other gauge bosons and probably depletes the WBF channel as well.

VI. CONCLUSIONS

In the $SO(5 \otimes U(1))$ gauge-Higgs unification model, in the Randall-Sundrum spacetime proposed in Ref. [4], the four-dimensional Higgs field becomes a part of the fifth-dimensional component of the gauge fields. Electroweak symmetry is broken dynamically through loop corrections to the Higgs potential and the conservation of an additional quantum number called H parity renders absolute stability to the Higgs boson which becomes a natural cold dark matter candidate. As a consequence of vanishing of all triple couplings to the standard model spectrum by virtue of H-parity conservation, the Higgs boson can only be produced in pairs through quartic couplings to massive gauge bosons and fermions. The mass of such a Higgs dark matter is constrained from recent astrophysical data to lie in the 70–90 GeV mass range.

In this paper, we show that for an $\mathcal{O}(1$ TeV) KK mass scale the 14 TeV LHC has the potential to discover such a Higgs dark matter particle of 70(90) GeV mass with 255(257 fb^{-1}) of integrated luminosity for a 5σ observation in the weak boson fusion channel following the same

search strategy used in the single invisibly decaying Higgs case of Ref. [9]. On the other hand, the cut on the azimuthal angle between the tagging jets proposed in Ref. [9] to reduce the SM WBF backgrounds were found to be less effective from the point of view of reducing the amount of data necessary for discovery compared to the single Higgs case, which demonstrates that there is still room for optimization of the search strategy.

As a final comment, the enhanced production cross section compared to the SM case is due the lack of cancellations between the triple and quartic contributions to the double Higgs production. This feature may help to establish the model if the growth of the vector boson scattering amplitudes as a function of the energy could be determined, for example, in a future linear collider or in the LHC, using dedicated methods to that aim as, for example, was proposed in [20].

ACKNOWLEDGMENTS

We would like to thank Oscar Éboli for reading the manuscript and encouragement. This research was supported by Conselho Nacional de Desenvolvimento Científico e Tecnológico (CNPq).

[1] See for example: W. Killian, *Electroweak Symmetry Breaking* (Springer, New York, 2005).
[2] For a very complete Higgs boson phenomenology review see A. Djouadi, Phys. Rep. **457**, 1 (2008), andA. Djouadi Phys. Rep. **459**, 1 (2008).
[3] J. Dunkley *et al.* (WMAP Collaboration), Astrophys. J. Suppl. Ser. **180**, 306 (2009).
[4] Y. Hosotani, K. Oda, T. Ohnuma, and Y. Sakamura, Phys. Rev. D **78**, 096002 (2008); **79**, 079902(E) (2009); Y. Hosotani and Y. Kobayashi, Phys. Lett. B **674**, 192 (2009); Y. Hosotani, arXiv:1003.3129; Y. Hosotani, P. Ko, and M. Tanaka, Phys. Lett. B **680**, 179 (2009).
[5] K. Cheung, J. Song, and Po-Yan Tseng, arXiv:1007.0282.
[6] For reviews of supersymmetry, see for example: S. P. Martin, arXiv:hep-ph/9709356; I. J. R. Aitichson, arXiv:hep-ph/0505105.
[7] H. -C. Cheng, K. T. Matchev, and M. Schmaltz, Phys. Rev. D **66**, 056006 (2002).
[8] K. Cheung and J. Song, Phys. Rev. D **81**, 097703 (2010); **81**, 119905(E) (2010).
[9] O. Éboli and D. Zeppenfeld, Phys. Lett. B **495**, 147 (2000).
[10] V. D. Barger *et al.*, Phys. Rev. D **44**, 2701 (1991); **48**, 5444 (E) (1993); D. Rainwater and D. Zeppenfeld, J. High Energy Phys. 12 (1997) 005; D. Rainwater and D. Zeppenfeld, Phys. Rev. D **60**, 113004 (1999); **61**, 099901(E) (2000); N. Kauer, T. Plehn, D. Rainwater, and D. Zeppenfeld, Phys. Lett. B **503**, 113 (2001); K. Hagiwara, D. Rainwater, and D. Zeppenfeld, Phys. Rev. D **59**, 014037 (1998); T. Plehn, D. Rainwater, and D. Zeppenfeld, Phys. Rev. D **61**, 093005 (2000); C. Buttar, R. Harper, and K. Jakobs, Report No. ATL-PHYS-2002-033.
[11] T. Plehn, D. Rainwater, and D. Zeppenfeld, Phys. Lett. B **454**, 297 (1999).
[12] A. Alves, O. Éboli, T. Plehn, and D. Rainwater, Phys. Rev. D **69**, 075005 (2004); A. Dedes, T. Figy, S. Hoeche, F. Krauss, and T. E. J. Underwood, J. High Energy Phys. 11 (2008) 036.
[13] N. Haba, Y. Sakamura, and T. Yamashita, J. High Energy Phys. 03 (2010) 069; N. Haba, Y. Sakamura, and T. Yamashita, J. High Energy Phys. 07 (2009) 020.
[14] A. Pukhov, arXiv:hep-ph/0412191.
[15] T. Stelzer and F. Long, Comput. Phys. Commun. **81**, 357 (1994); F. Maltoni and T. Stelzer, J. High Energy Phys. 02 (2003) 027.
[16] T. Figy, Mod. Phys. Lett. A **23**, 1961 (2008).
[17] V. Barger, K. Cheung, T. Han, and R. J. N. Phillips, Phys. Rev. D **42**, 3052 (1990).
[18] H. L. Lai *et al.*, Phys. Rev. D **55**, 1280 (1997).
[19] D. Rainwater, Ph.D. thesis, Wisconsin University, Madison, 1999, arXiv:hep-ph/9908378.
[20] T. Han, D. Krohn, Lian-Tao Wang, and W. Zhu, J. High Energy Phys. 03 (2010) 082.
[21] J. M. Butterworth, B. E. Cox, and J. R. Forshaw, Phys. Rev. D **65**, 096014 (2002).
[22] G. -C. Cho, K. Hagiwara, J. Kanzaki, T. Plehn, D. Rainwater, and T. Stelzer, Phys. Rev. D **73**, 054002 (2006).